14th International Conference on Information Fusion
Chicago, Illinois, USA, July 5-8, 2011

A Box Particle Filter for Stochastic and Set-theoretic Measurements with Association Uncertainty

Amadou Gning
School of Computing & Communications
Lancaster University, InfoLab21
Lancaster
United Kingdom
e.gning@lancaster.ac.uk

Branko Ristic
ISR Division
DSTO
Melbourne
Australia
branko.ristic@dsto.defence.gov.au

Lyudmila Mihaylova
School of Computing & Communications
Lancaster University, InfoLab21
Lancaster
United Kingdom
mila.mihaylova@lancaster.ac.uk

***Abstract*—This work develops a novel estimation approach for nonlinear dynamic stochastic systems by combining the sequential Monte Carlo method with interval analysis. Unlike the common pointwise measurements, the proposed solution is for problems with interval measurements with association uncertainty. The optimal theoretical solution can be formulated in the framework of random set theory as the Bernoulli filter for interval measurements. The straightforward particle filter implementation of the Bernoulli filter typically requires a huge number of particles since the posterior probability density function occupies a significant portion of the state space.**

In order to reduce the number of particles, without necessarily sacrificing estimation accuracy, the paper investigates an implementation based on box particles. A box particle occupies a small and controllable rectangular region of non-zero volume in the target state space. The numerical results demonstrate that the filter performs remarkably well: both target state and target presence are estimated reliably using a very small number of box particles.

***Index Terms*—Sequential Bayesian Estimation, Box Particle filters, Detection, Random Sets, Interval Measurements.**

I. Introduction

Traditionally, the measurements used for nonlinear filtering are points in the measurement space, typically affected by additive measurement noise of a known probability density function (PDF) [2]. The traditional measurements express uncertainty only due to randomness, often referred to as statistical or stochastic uncertainty. In many practical applications, however, the measurements are know within certain intervals. In sensor networks, for example, in order to reduce the communication bandwidth, the measurements are quantized to only a few bits. Such measurements represent intervals rather than point values. The intervals express a type of uncertainty which is referred to as the set-theoretic uncertainty [3], vagueness [4] or imprecision [5]. The importance and distinctness of this type of uncertainty have been well recognised by the researchers in expert systems [6]. In the context of Bayes filtering, set-theoretic uncertainty is convenient for modeling bounded errors with unknown distributions and unknown measurement biases. The two types of uncertainties, the set-theoretic and stochastic, can be treated in combination using various modern formalisms, such as: the set of densities [7], imprecise probabilities [8] or random sets [1].

Often, a third source of uncertainty in measurements is also present. This is uncertainty due to the measurement origin, which is a consequence of imperfections in the detection process. Sensor measurements are typically characterised by the probability of detection less than one, and with a certain false detection rate [9]. This translates into uncertainty as to which (if any) of the received measurements is due to the target (the so called data association uncertainty).

The theoretical formulation of the optimal Bayes nonlinear filter for the measurements affected by the three discussed sources of uncertainty (stochastic, set-theoretic and association uncertainty) has been carried out in the accompanying paper [23]. Using Mahler's framework for information fusion [1], the solution is formulated as the Bernoulli filter for interval measurements. The straightforward particle filter implementation of the Bernoulli filter typically requires a huge number of particles since the posterior probability density function occupies a significant portion of the state space. In order to overcome this problem, the present paper proposes a novel and very efficient implementation of the Bernoulli filter for interval measurements. The proposed solution combines the interval analysis approach with sequential Monte Carlo methods, known as particle filters [12].

Particle filters have emerged as a powerful tool for solving complex problems, with nonlinearities and non-Gaussian noises. However, for high dimensional systems, the complexity of the sequential Monte Carlo methods increases significantly. Lead by the motivation to reduce the computational load, the concept of a *box particle* was proposed in [17]. A box particle occupies a small and controllable rectangular region of non-zero volume in the target state space. Nonlinear filtering using box particles (the so-called *box particle filter*) relies on methods and techniques developed in the field of interval analysis, see [19]. A theoretical justification of the box particle filter is given in [18], based on the concept that the posterior state PDF can be represented by a mixture of uniform distributions with box supports. In the present paper we propose a novel box particle filter which is a combination of the Bernoulli particle filter [23] with the box particle filter [17], [18]. The new filter is referred to as the Box Bernoulli Particle filter. The paper illustrates the usefulness and the efficiency of the proposed approach by a numerical example with set measurement uncertainties.

The paper is organised as follows. The formal description of the problem is given in Sec. II. Section III briefly presents interval analysis principles and relevant tools for non linear filtering are introduced. Next, the Bernoulli filter is described in Section IV. A box particle filter implementation is presented in Section V. Numerical studies are presented in Section VI and finally the conclusions are drawn in Section VII.

II. Problem description

The state vector of the dynamic system (target) at discrete time k is denoted by $\mathbf{x}_k$; it takes values from the state space $\mathcal{X} \subseteq \mathbb{R}^{n_x}$. The target, however, may or may not be present in the surveillance region at a particular time t_k. We therefore model the object state at discrete-time k by a finite set $\mathbf{X}_k$ which can be either empty or a singleton. Mahler's *finite set statistics* (FISST) provides practical tools for mathematical manipulations of finite-set random variables, including the concept of probability density function and its integral [1].

A convenient model of target state at time k is the Bernoulli random finite set (RFS) on $\mathcal{X}$. A Bernoulli RFS $\mathbf{X}$ is defined by a parameters q and a PDF $s(.)$ defined on $\mathcal{X}$. The RFS $\mathcal{X}$ has a probability $1-q$ of being empty and a probability q of being a singleton whose only element is distributed according to the PDF $s(.)$. The FISST probability density of a Bernoulli RFS $\mathbf{X}$ is defined as

$$f(\mathbf{X}) = \begin{cases} 1-q, & \text{if } \mathbf{X} = \emptyset \\ q \cdot s(\mathbf{x}), & \text{if } \mathbf{X} = \{\mathbf{x}\} \\ 0, & \text{otherwise} \end{cases}. \tag{1}$$

The objective of Bayes filtering is to sequentially estimate $\mathbf{X}_k$ from measurements collected up to time k. Suppose the measurement set at time k is denoted by $\mathbf{\Upsilon}_k$. Then formally the goal is to estimate sequentially the posterior PDF $f_{k|k}(\mathbf{X}|\mathbf{\Upsilon}_{1:k})$ of a Bernoulli random finite process, where $\mathbf{\Upsilon}_{1:k} = (\mathbf{\Upsilon}_1, \dots, \mathbf{\Upsilon}_k)$ denotes the set of up to time k. The estimation process is based on prior knowledge of two models, the *target dynamics model* and the *measurement model*.

A. Target dynamics model

The target dynamic model is defined by the probability density $\phi_{k+1|k}(\mathbf{X}|\mathbf{X}')$ associated with moving from state $\mathbf{X}'$ at time k to $\mathbf{X}$ at time $k+1$. Since both $\mathbf{X}'$ and $\mathbf{X}$ are Bernoulli RFSs, $\phi_{k+1|k}(\mathbf{X}|\mathbf{X}')$ can be defined as:

$$\phi_{k+1|k}(\mathbf{X}|\mathbf{X}') = \begin{cases} 1-p_B, & \text{if } \mathbf{X}' = \emptyset, \mathbf{X} = \emptyset \\ p_B \cdot b_{k+1|k}(\mathbf{x}), & \text{if } \mathbf{X}' = \emptyset, \mathbf{X} = \{\mathbf{x}\} \\ 1-p_S(\mathbf{x}'), & \text{if } \mathbf{X}' = \{\mathbf{x}'\}, \mathbf{X} = \emptyset \\ p_S(\mathbf{x}') \cdot \pi_{k+1|k}(\mathbf{x}|\mathbf{x}'), & \text{if } \mathbf{X}' = \{\mathbf{x}'\}, \mathbf{X} = \{\mathbf{x}\} \end{cases}, \tag{2}$$

where

- $p_B \overset{\text{abbr}}{=} p_{B,k+1|k}$ is the probability of target *birth* during the time interval from k to $k+1$;
- $b_{k+1|k}(\mathbf{x})$ is the spatial distribution of target birth during the time interval from k to $k+1$;
- $p_S(\mathbf{x}') \overset{\text{abbr}}{=} p_{S,k+1|k}(\mathbf{x}')$ is the probability that a target with state $\mathbf{x}'$ at time k will survive until time $k+1$;
- $\pi_{k+1|k}(\mathbf{x}|\mathbf{x}')$ is the target transition density from time k to $k+1$.

In the paper we assume that the transition density is Gaussian, that is $\pi_{k+1|k}(\mathbf{x}|\mathbf{x}') = \mathcal{N}(\mathbf{x}; \psi_k(\mathbf{x}'), \mathbf{Q})$, where $\mathbf{Q}$ is a known process noise covariance matrix and the function ψ_k is a known deterministic mapping from the state space $\mathcal{X}$ to itself.

B. Measurement model

In general, target detection is imperfect: a target may not be detected at scan k, whereas a set of non-existent objects may be detected and reported (false detections or clutter). Let the measurement space be denoted $\mathcal{Z} \subseteq \mathbb{R}^{n_z}$. If a target exists, i.e. $\mathbf{X}_k = \{\mathbf{x}\}$, and has been detected, the conventional point measurement $\mathbf{z} \in \mathcal{Z}$ is related to the target state via a nonlinear equation:

$$\mathbf{z} = h_k(\mathbf{x}) + \mathbf{v}, \tag{3}$$

where the function h_k is a known deterministic mapping from the state space $\mathcal{X}$ to the measurement space $\mathcal{Z}$, while $\mathbf{v}$ is a measurement noise vector characterised by PDF $p_{\mathbf{v}}$.

In this paper we assume that if a target exists ($\mathbf{x} \in \mathbf{X}_k$) and is detected, the sensor does not report the conventional measurement $\mathbf{z} \in \mathcal{Z}$¿ Instead, it reports a closed interval $[\mathbf{z}] \subset \mathcal{Z}$ such that the target originated measurement (3) satisfies $p(h_k(\mathbf{x}) \in [\mathbf{z}]) = 1$. Let us denote by $\mathcal{IZ}$ the set of all such closed intervals. Note that interval measurements $[\mathbf{z}]$ represent a special case of what Mahler [1] refers to as unambiguously generated ambiguous (UGA) measurements. More general instances of UGA measurements include mixtures of fuzzy membership functions, referred to as fuzzy Dempster-Shafer evidence.

Due to the imperfect detection process, $m_k \geq 0$ interval measurements $[\mathbf{z}]_{k,1}, \dots, [\mathbf{z}]_{k,m_k}$ are collected at time k. The measurements can be represented by a finite set:

$$\mathbf{\Upsilon}_k = \{[\mathbf{z}]_{k,1}, \dots, [\mathbf{z}]_{k,m_k}\} \in \mathcal{F}(\mathcal{IZ}), \tag{4}$$

where $\mathcal{F}(\mathcal{IZ})$ is the space of finite subsets of $\mathcal{IZ}$.

The probability of target detection can be state independent and is denoted as $p_D(\mathbf{x})$. The false detections are assumed to be independent of the target state. The number of false detections per scan is modeled by a Poisson distribution with mean λ; the spatial distribution of false detections is modeled by a PDF $c([\mathbf{z}])$.

The measurement set $\boldsymbol{\Upsilon}_k$ is characterised by three sources of uncertainty. Additive noise $\mathbf{v}$ in (3) is the source of stochastic uncertainty. The target originated interval measurement $[\mathbf{z}]$ is non-specific and as such is the source of imprecision. Finally, the existence of false detections and a possible absence of target originated detection is the source of data association uncertainty.

III. Elements of Interval Analysis

A real interval, $[x] = [\underline{x},\ \overline{x}]$ is defined as a closed and connected subset of the set $\mathbb{R}$ of real numbers. In a vector form, a box $[\mathbf{x}]$ of $\mathbb{R}^{n_x}$ is defined as a Cartesian product of n_x intervals: $[\mathbf{x}] = [x_1] \times [x_2] \cdots \times [x_n] = \times_{i=1}^{n_x}[x_i]$. In this paper, the operator $|[.]|$ denotes the size $|[\mathbf{x}]|$ of a box $[\mathbf{x}]$. The underlying concept of interval analysis is to deal with intervals of real numbers instead of dealing with real numbers. For that purpose, elementary arithmetic operations, e.g., $+, -, *, \div$, etc., as well as operations between sets of $\mathbb{R}^n$, such as $\subset, \supset, \cap, \cup$, etc., have been naturally extended to interval analysis context.

In addition, a lot of research has been performed with the so called *inclusion functions* [19]. An *inclusion function* $[f]$ of a given function f is defined such that the image of a box $[\mathbf{x}]$ is a box $[f]([\mathbf{x}])$ containing $f([\mathbf{x}])$. The goal of inclusion functions is to work only with intervals, to optimise the interval enclosing the real image set and, then to decrease the pessimism when intervals are propagated.

Often constraints have to be fulfilled which requires to solve the *Constraint Satisfaction Problems* (CSPs). A CSP often denoted $\mathcal{H}$ can be written:

$$\mathcal{H} : (\mathbf{f}(\mathbf{x}) = \mathbf{0}, \mathbf{x} \in [\mathbf{x}]). \tag{5}$$

Equation (5) can be interpreted as follows: find the optimal box enclosure of the set of vector $\mathbf{x}$ belonging to a given prior domain $[\mathbf{x}] \subset \mathbb{R}^n$ satisfying a set of m constraints $\mathbf{f}$ (with $\mathbf{f}$ a multivalued function, i.e., $\mathbf{f} = (f_1, f_2, \cdots, f_m)^T$, where the f_i are real valued functions). The solution set of $\mathcal{H}$ is defined as:

$$\mathcal{S} = \{\mathbf{x} \in [\mathbf{x}] \mid \mathbf{f}(\mathbf{x}) = \mathbf{0}\}. \tag{6}$$

Contracting $\mathcal{H}$ means replacing $[\mathbf{x}]$ by a smaller domain $[\mathbf{x}]'$ such that $\mathcal{S} \subseteq [\mathbf{x}]' \subseteq [\mathbf{x}]$. A *contractor* for $\mathcal{H}$ is any operator that can be used to contract $\mathcal{H}$. Several methods for building contractors are described in [19, Chapter 4], including Gauss elimination, the Gauss-Seidel algorithm, linear programming, etc. Each of these methods may be more suitable to some types of CSP. Although the approaches presented in this work are not limited to any particular contractor, a general and well known contraction method, the *Constraints Propagation* (CP) technique is used in this paper. The main advantages of the CP method is its efficiency in the presence of high redundancy of data and equations. The CP method is also known to be simple and, most importantly, to be independent of nonlinearities.

IV. Bernoulli filter

The optimal Bayes filter for the problem described above is the Bernoulli filter [1, Section 14.7], [10] for interval measurements. Let $f_{k|k}(\mathbf{X}|\boldsymbol{\Upsilon}_{1:k})$ denote the posterior PDF of Bernoulli RFS $\mathbf{X}$ at k. The propagation of this posterior over time is carried out in two steps, the *prediction* and *update*. We have seen that $f_{k|k}(\mathbf{X}|\boldsymbol{\Upsilon}_{1:k})$ is completely defined by two posteriors: $q_{k|k} = Pr\{|\mathbf{X}_k| = 1 \mid \boldsymbol{\Upsilon}_k\}$ is[1] the posterior probability of target existence, while $s_{k|k}(\mathbf{x}) = p(\mathbf{x}_k|\boldsymbol{\Upsilon}_{1:k})$ is the posterior spatial PDF of $\mathbf{X}_k = \{\mathbf{x}\}$. The Bernoulli filter requires only these two quantities to be propagated.

A. Equations

Assuming that p_S is state independent, the prediction step equations are given by:

$$q_{k+1|k} = p_B \cdot (1 - q_{k|k}) + p_S \cdot q_{k|k} \tag{7}$$

$$s_{k+1|k}(\mathbf{x}) = \frac{p_B \cdot (1 - q_{k|k}) b_{k+1|k}(\mathbf{x})}{q_{k+1|k}} + \frac{p_S\, q_{k|k} \int \pi_{k+1|k}(\mathbf{x}|\mathbf{x}') \cdot s_{k|k}(\mathbf{x}')\, d\mathbf{x}'}{q_{k+1|k}}. \tag{8}$$

The predicted birth density $b_{k+1|k}(\mathbf{x})$ in general is unknown and needs to be adaptively designed using the measurement set $\boldsymbol{\Upsilon}_k$ from the previous scan k. This is further discussed in Section V.

Assuming p_D is constant over the state-space $\mathcal{X}$, the update equations of the Bernoulli filter for interval measurements are as follows [1, Section 14.7]. The probability of existence is updated using the measurement set $\boldsymbol{\Upsilon}_{k+1}$ as:

$$q_{k+1|k+1} = \frac{1 - \delta_{k+1}}{1 - \delta_{k+1} \cdot q_{k+1|k}} \cdot q_{k+1|k}, \tag{9}$$

where

$$\delta_{k+1} = p_D \left(1 - \sum_{[\mathbf{z}] \in \boldsymbol{\Upsilon}_{k+1}} \frac{\int g_{k+1}([\mathbf{z}]|\mathbf{x})\, s_{k+1|k}(\mathbf{x})\, d\mathbf{x}}{\lambda\, c([\mathbf{z}])} \right). \tag{10}$$

Here $g_{k+1}([\mathbf{z}]|\mathbf{x})$ is the *generalised* likelihood function at $k+1$ for a target originated interval measurement. Furthermore λ and $c([\mathbf{z}])$ are already defined clutter parameters. The generalised likelihood will be further discussed in Section V-B.

The target spatial PDF is updated as follows:

$$s_{k+1|k+1}(\mathbf{x}) = \frac{1 - p_D + p_D \sum_{[\mathbf{z}] \in \boldsymbol{\Upsilon}_{k+1}} \frac{g_{k+1}([\mathbf{z}]|\mathbf{x})}{\lambda c([\mathbf{z}])}}{1 - \delta_{k+1}}\, s_{k+1|k}(\mathbf{x}). \tag{11}$$

In the special case where the detection process is perfect, i.e. $p_D = 1$ and no false detections, the measurement set becomes a singleton $\boldsymbol{\Upsilon}_{k+1} = \{[\mathbf{z}]\}$, containing only the target originated measurement. Then it is easy to verify that $\lambda c([\mathbf{z}])$ terms cancel out in (9) and (11) and with $p_B = 0$, $p_S = 1$, the Bernoulli filter for interval measurements becomes identical to the Bayes filter for interval measurements [1, p.159]. For

[1] $|\mathbf{X}|$ denotes the cardinality of set $\mathbf{X}$.

the more general case of $p_D(\mathbf{x})$ and $p_S(\mathbf{x})$, the Bernoulli filter equations can be found in [1, Sec.14.7].

Remark 1: The proposed Bernoulli filter is the optimal Bayes filter for the considered problem. Moreover, it is directly applicable to multi-sensor tracking and fusion (unlike for example the PHD filter [11]). While the Bernoulli filter is a single-target tracking algorithm, it can be used in multi-target applications by treating each target separately and by including an appropriate data association technique when targets become close to each other.

V. Box Particle Filter Implementation

In general there is no analytic solution for the Bernoulli filter (equations (8)-(11)). Particle filters have become a popular class of numerical methods for implementation of Bayes filters [12], [13], both in the context of single and multiple targets [1]. When this method is applied to the Bernoulli filter, the resulting Bernoulli particle filter approximates the spatial PDF[2] $s_{k|k}(\mathbf{x})$ by a set of N weighted random samples or particles $\{w_k^i, \mathbf{x}_k^i\}_{i=1}^N$, where $\mathbf{x}_k^i$ is the state of particle i and w_k^i is its corresponding normalised weight, such that $\sum_{i=1}^N w_k^i = 1$. The approximation of $s_{k|k}(\mathbf{x})$ can be written as

$$s_{k|k}(\mathbf{x}) \approx \sum_{i=1}^{N} w_k^i \, \delta_{\mathbf{x}_k^i}(\mathbf{x}), \tag{12}$$

where $\delta_{\mathbf{x}_k^i}(\mathbf{x})$ denote the Dirac delta function concentrated at $\mathbf{x}_k^i$. For an appropriately chosen importance density, the sum in (12) converges to $s_{k|k}(\mathbf{x})$ as $N \to \infty$ [14].

For some applications, the number N of particles to use is a key issue since it may lead to a computationally demanding filter. For instance, if the posterior PDFs to be estimated are with very large supports, the number of particles has to be chosen to be very large in order to explore a significant part of the state space. One natural solution to reduce N is the use of box particles [17]. The point particles are replaced with box particles since they have the attractive property to cover any prior region with far less boxes. In [17], the efficiency of box particles combined with interval analysis tools [19] is demonstrated. Furthermore, in [18] it is also shown that box particles can be interpreted as being supports of uniform PDFs, and in this respect, (12) becomes:

$$s_{k|k}(\mathbf{x}) \approx \sum_{i=1}^{N} w_k^i \, U_{[\mathbf{x}_k^i]}(\mathbf{x}), \tag{13}$$

where $U_{[\mathbf{x}_k^i]}$ denotes the uniform PDF over the box $[\mathbf{x}_k^i]$.

Staring from the posterior Bernoulli density at scan k, represented by $q_{k|k}$ and a set of weighted box particles $\{w_k^i, [\mathbf{x}_k^i]\}_{i=1}^N$, a cycle of the Bernoulli box particle filter for interval measurements is summarised in Algorithm1.

[2]Strictly speaking particle filters approximate integrals, not densities, [12], [13].

A. Prediction step

The implementation of the prediction equation (8) requires to use box particles samples approximation for two densities. First, the predicted birth density $b_{k+1|k}(\mathbf{x})$ is implemented as:

$$b_{k+1|k}(\mathbf{x}) = \int \pi_{k+1|k}(\mathbf{x}|\boldsymbol{\xi}) \, b_k(\boldsymbol{\xi}) \, d\boldsymbol{\xi}, \tag{14}$$

where $b_k(.)$ is the birth density at the previous time step k. If the target can appear anywhere in the state space $\mathcal{X}$, an obvious choice for $b_k(\mathbf{x})$ is the uniform density over $\mathcal{X}$. This, however, would not take into account the fact that the previous time measurements are likely to contain information about birth targets. Consequently $b_k(.)$ is designed adaptively, using the measurement set from the previous scan k, $\boldsymbol{\Upsilon}_k$, i.e.

$$b_k(\mathbf{x}) \approx \frac{1}{|\boldsymbol{\Upsilon}_k|} \sum_{[\mathbf{z}] \in \boldsymbol{\Upsilon}_k} \beta(\mathbf{x}|[\mathbf{z}]). \tag{15}$$

The densities $\beta(\mathbf{x}|[\mathbf{z}])$ in the mixture (15) are also approximated with a mixture of uniform PDFs compatible with the interval measurement $[\mathbf{z}] \in \boldsymbol{\Upsilon}_k$ i.e.

$$\beta(\mathbf{x}|[\mathbf{z}]) \approx \frac{1}{n_0} \sum_{i=1}^{n_0} U_{[\mathbf{x}_{b,k}^i]}(\mathbf{x}). \tag{16}$$

Equations (15) and (16) mean that $b_k(.)$ is represented by a set of N_b box particles $\{[\mathbf{x}_{b,k}^i]\}_{i=1}^{N_b}$. The number of newborn particles depends on the cardinality of $\boldsymbol{\Upsilon}_k$, that is $N_b = |\boldsymbol{\Upsilon}_k| \cdot n_0$, where n_0 is a design parameter. In (16), to sample the n_0 box particles $\{[\mathbf{x}_{b,k}^i]\}_{i=1}^{n_0}$, a reciprocal set $[h_k^{-1}]([\mathbf{z}])$ of $[\mathbf{z}]$ has first to be calculated. Then, $[h_k^{-1}]([\mathbf{z}])$ is subdivided into n_0 boxes. The weights associated with the newborn box particles are made equal, i.e. $w_{b,k}^i = 1/N_b$ for $i = 1, \ldots, N_b$. Box particles are drawn from $b_k(\mathbf{x})$ in Step 4 of Algorithm 1.

Two clouds of weighted box particles, the "persistent" $\{w_{p,k}^i, [\mathbf{x}_{p,k}^i]\}_{i=1}^N$ and the "newborn" box particles $\{w_{b,k}^i, [\mathbf{x}_{b,k}^i]\}_{i=1}^{N_b}$, are used to approximate the predicted spatial PDF of (8). The summation of the two terms on the right-hand side of (8) is carried out by the union of these two sets of particles (Step 7 in Algorithm1). The number of predicted particles is then $N' = N + N_b$. It is shown in [18] that each of these two terms representing the newborn and persistent box particles can be approximated with box particles according to:

$$\begin{aligned} b_{k+1|k}(\mathbf{x}) = & \int \pi_{k+1|k}(\mathbf{x}|\boldsymbol{\xi}) \, b_k(\boldsymbol{\xi}) \, d\boldsymbol{\xi} \\ \approx & \quad w_{b,k}^i \textstyle\sum_{i=1}^{N_b} U_{[\psi_k]([\mathbf{x}_{b,k}^i])}(\mathbf{x}), \end{aligned} \tag{17}$$

$$\int \pi_{k+1|k}(\mathbf{x}|\boldsymbol{\xi}) \cdot s_{k|k}(\boldsymbol{\xi}) \, d\boldsymbol{\xi} \approx \quad w_k^i \textstyle\sum_{i=1}^{N} U_{[\psi_k]([\mathbf{x}_{p,k}^i])}(\mathbf{x}). \tag{18}$$

Equations (17) and (18) mean that the predicted PDF $s_{k+1|k}(.)$ can be approximated using the set of weighted box particles $\{w_{k+1|k}^i, [\mathbf{x}_{k+1|k}^i]\}_{i=1}^{N'}$ constituted of the weighted box particles $\{w_{p,k+1}^i, [\psi_k]([\mathbf{x}_{p,k}^i])\}_{i=1}^N$ and $\{w_{b,k+1}^i, [\psi_k]([\mathbf{x}_{b,k}^i])\}_{i=1}^{N_b}$. The weights $\{w_{p,k+1}^i\}_{i=1}^N$ and $\{w_{b,k+1}^i\}_{i=1}^{N_b}$ are computed according to (8), see Step 6 in Algorithm1.

Algorithm 1: The steps of the box Bernoulli particle filter for interval measurements

1: **Input**: $q_{k|k}$, $\{w_k^i, \mathbf{x}_k^i\}_{i=1}^N$, $\mathbf{\Upsilon}_k$, $\mathbf{\Upsilon}_{k+1}$;

Prediction

2: Compute $q_{k+1|k}$ using (7)

3: Propagate *persistent* box particles at $k+1$: $[\mathbf{x}_{p,k+1}^i] = [\psi_{k+1}]([\mathbf{x}_k^i])$ for $i = 1, \ldots, N$

4: Create a weighted set of *newborn* box particles $\{w_{b,k}^i, [\mathbf{x}_{b,k}^i]\}_{i=1}^{N_b}$ at k from birth density $b_k(\mathbf{x})$ defined by (15) using $\mathbf{\Upsilon}_k$, with $w_{b,k}^i = 1/N_b$;

5: Propagate *newborn* particles at $k+1$: $[\mathbf{x}_{b,k+1}^i] = [\psi_{k+1}]([\mathbf{x}_{b,k}^i])$ for $i = 1, \ldots, N_b$

6: Compute the box particle prediction weights at $k+1$:

$$\begin{aligned} w_{p,k+1}^i &= p_S\, q_{k|k}\; w_k^i / q_{k+1|k}; \qquad \text{for } i = 1, \ldots, N \\ w_{b,k+1}^i &= p_B\,(1 - q_{k|k}) w_{b,k}^i / q_{k+1|k}; \quad \text{for } i = 1, \ldots, N_b \end{aligned}$$

7: Union of weighted box particles: $\{w_{k+1|k}^i, [\mathbf{x}_{k+1|k}^i]\}_{i=1}^{N'} = \{w_{b,k+1}^i, [\mathbf{x}_{b,k+1}^i]\}_{i=1}^{N_b} \cup \{w_{p,k+1}^i, [\mathbf{x}_{p,k+1}^i]\}_{i=1}^{N}$, where $N' = N + N_b$;

Update

8: Replicate the box particle $[\mathbf{x}_{k+1|k}^i]$ to obtain N' box particle $\tilde{\mathbf{x}}_{k+1}^i$ with weights $[\tilde{w}_{k+1}^i] = (1 - p_D) w_{k+1|k}^i$

9: For every box particle $[\mathbf{x}_{k+1|k}^i]$, $i = 1, \ldots, N'$ and every measurement $[\mathbf{z}] \in \mathbf{\Upsilon}_{k+1}$,

- use a contraction algorithm according to (24) to obtain a new box particle $[\tilde{\mathbf{x}}_{k+1}^i]$;
- compute the weight $\tilde{w}_{k+1}^i$ of $[\tilde{\mathbf{x}}_{k+1}^i]$ according to (26);

10: Compute δ_{k+1} according to (10) and (28);

11: Compute $q_{k+1|k+1}$ according to (9);

12: Normalise weights: $\tilde{w}_{k+1}^i = \tilde{w}_{k+1}^i / \sum_{j=1}^{N'(1+m_k)} \tilde{w}_{k+1}^j$;

13: Resample N times from $\{\tilde{w}_{k+1}^i, [\mathbf{x}_{k+1|k}^i]\}_{i=1}^{N'(1+m_k)}$ to obtain N equally weighted box particles $\{w_{k+1}^i = \frac{1}{N}, [\mathbf{x}_{k+1}^i]\}_{i=1}^N$

14: **Output**: $q_{k+1|k+1}$, $\{w_{k+1}^i, [\mathbf{x}_{k+1}^i]\}_{i=1}^N$

B. Generalised Likelihood Function

The update equations (9) and (11) are different from the standard Bayesian filters since the standard measurement likelihood function is replaced by the *generalised* likelihood function $g_k([\mathbf{z}]|\mathbf{x})$. Furthermore, in [18], it is shown that the BPF update step requires contraction steps in addition to the likelihood factors calculation. Here, in addition to a stochastic noise assumed in [18], the measurements are assumed to be perturbed by both uncertainty and set theoretic noise. If $[\mathbf{z}] \in \mathbf{\Upsilon}_k$ and $\mathbf{x}$ a box in $\mathbf{X}_k$, the generalised likelihood funtion is defined as follows:

$$\begin{aligned} g_k([\mathbf{z}]|\mathbf{x}) &\overset{\text{def}}{=} Pr\{h_k(\mathbf{x}) + \mathbf{v} \in [\mathbf{z}]\} \\ &= \int_{[\mathbf{z}]} p_{\mathbf{v}}(\mathbf{z} - h_k(\mathbf{x}))\, d\mathbf{z}. \end{aligned} \tag{19}$$

Assume that the stochastic uncertainty (which is due to the measurement noise $\mathbf{v}$) is small. One can adopt the following approximation using a uniform PDF: [1, p.101]:

$$p_{\mathbf{v}}(\mathbf{v}) \approx U_{[\boldsymbol{\varepsilon}]}(\mathbf{v}), \tag{20}$$

where $[\boldsymbol{\varepsilon}]$ is the measurement noise support. Using the approximation (20) in (19) results in:

$$\begin{aligned} g_k([\mathbf{z}]|\mathbf{x}) &\approx \int_{[\mathbf{z}]} U_{[\boldsymbol{\varepsilon}]}(\mathbf{z} - h_k(\mathbf{x}))\, d\mathbf{z} \\ &= \frac{|\,[\mathbf{z}] \cap (h_k(\mathbf{x}) + [\boldsymbol{\varepsilon}])\,|}{|[\boldsymbol{\varepsilon}]|}. \end{aligned} \tag{21}$$

Here $|.|$ denotes the Lebesgue measure operator (e.g. the volume for boxes in 3D). From (19) we can see that

$$g_k([\mathbf{z}]|\mathbf{x}) \approx \begin{cases} 1, & \text{if } h_k(\mathbf{x}) + [\boldsymbol{\varepsilon}] \subseteq [\mathbf{z}] \\ 0, & \text{if } h_k(\mathbf{x}) + [\boldsymbol{\varepsilon}] \cap [\mathbf{z}] = \emptyset\ . \\ \leq 1, & \text{otherwise} \end{cases} \tag{22}$$

Remark 2: In the general case, $p_{\mathbf{v}}$ cannot be approximated with a single uniform PDF but can be appropriately approximated using a mixture of uniform PDFs. It can be seen that a weighted sum of terms in the form of the fraction in (21) can be used to approximate the generalised likelihood function for a more general expression of the noise PDF $p_{\mathbf{v}}$. For simplicity the expression (19) of the generalised likelihood is considered for the rest of the paper and for each time instant k, $p_{\mathbf{v}}$ is approximated by $U_{[\boldsymbol{\varepsilon}_k]}$.

C. Update step

The update equations of the Bernoulli box particle filter are implemented by steps 8-13 of Algorithm1. Using the box particles approximation $s_{k+1|k}(\mathbf{x}) \approx \sum_{i=1}^{N'} w_{k+1|k}^i\, U_{[\mathbf{x}_{k+1|k}^i]}(\mathbf{x})$, and the generalised likelihood (21), in (11) the terms $\frac{p_D}{c([\mathbf{z}])} \cdot$

$g_{k+1}([\mathbf{z}]|\mathbf{x}) \cdot s_{k+1|k}(\mathbf{x})$ can be written

$$\frac{p_D}{c([\mathbf{z}])} \cdot g_{k+1}([\mathbf{z}]|\mathbf{x}) \cdot s_{k+1|k}(\mathbf{x}) =$$
$$\frac{p_D}{c([\mathbf{z}])} \cdot \sum_{i=1}^{N'} w^i_{k+1|k} \frac{|\,[\mathbf{z}] \cap (h_k(\mathbf{x}) + [\boldsymbol{\varepsilon}_{k+1}])\,|}{|[\boldsymbol{\varepsilon}_{k+1}]|} U_{[\mathbf{x}^i_{k+1|k}]}(\mathbf{x}). \tag{23}$$

Similarly to what is theoretically derived in [18] for the case of point measurements, the supports of the terms inside the summation in the right-hand side in (23) can be approximated using contraction operations (see Section III). The exact supports are the set solution of :

$$\{\mathbf{x} \in [\mathbf{x}^i_{k+1|k}] | [\mathbf{z}] \cap (h_k(\mathbf{x}) + [\boldsymbol{\varepsilon}_{k+1}]) \neq \emptyset\}. \tag{24}$$

In Algorithm1, each term inside the summation in the right-hand side of (23) is approximated by a weighted single uniform PDFs $U_{[\mathbf{x}^i_{k+1}]}(\mathbf{x})$ i.e.

$$\frac{p_D}{c([\mathbf{z}])} \cdot g_{k+1}([\mathbf{z}]|\mathbf{x}) \cdot s_{k+1|k}(\mathbf{x}) \simeq \sum_{i=1}^{N'} \tilde{w}^i_{k+1} U_{[\tilde{\mathbf{x}}^i_{k+1}]}(\mathbf{x}), \tag{25}$$

where $[\tilde{\mathbf{x}}^i_{k+1}]$ is a box enclosure of the support (24) that can be obtained by a contraction algorithm. The new weights $\tilde{w}^i_{k+1}$ are obtained from (23) and they have the expression

$$\tilde{w}^i_{k+1} = \frac{p_D}{c([\mathbf{z}])} \cdot w^i_{k+1|k} \kappa^i_{k+1} \frac{|[\tilde{\mathbf{x}}^i_{k+1}]|}{|[\mathbf{x}^i_{k+1|k}]|}, \tag{26}$$

where κ^i_{k+1} is chosen to be the expectation of the generalised likelihood $g_{k+1}([\mathbf{z}]|\mathbf{x})$ over the box particle $[\tilde{\mathbf{x}}^i_{k+1}]$ and κ^i_{k+1} can be written:

$$\kappa^i_{k+1} = \frac{1}{|[\tilde{\mathbf{x}}^i_{k+1}]|} \int_{[\tilde{\mathbf{x}}^i_{k+1}]} \frac{|[\mathbf{z}] \cap (h_k(\mathbf{x}) + [\boldsymbol{\varepsilon}_{k+1}])|}{|[\boldsymbol{\varepsilon}_{k+1}]|} d\mathbf{x}. \tag{27}$$

The integral defining (27) is not known in a closed form but can be approximated (for instance by using a partition of the set $[\tilde{\mathbf{x}}^i_{k+1}]$ as it is done in the Riemann integration theory [22]).

Remark 3: here, bearing in mind Equation (11), the posterior PDF $s_{k+1}(.)$ at time instant $k+1$ is approximated using two new clouds of particles: N' particles $[\tilde{\mathbf{x}}^i_{k+1|k}]$ with weights $(1-p_D)\tilde{w}^i_{k+1|k}$ and $m_k \times N'$ particles obtained from the m_k measurements according to (25) and (26).

Next, in (10), the terms $\int g_{k+1}([\mathbf{z}]|\mathbf{x})\, s_{k+1|k}(\mathbf{x})\, d\mathbf{x}$ can be written as

$$\int g_{k+1}([\mathbf{z}]|\mathbf{x})\, s_{k+1|k}(\mathbf{x})\, d\mathbf{x} =$$
$$\int \frac{|\,[\mathbf{z}] \cap (h_{k+1}(\mathbf{x}) + [\boldsymbol{\varepsilon}_{k+1}])\,|}{|[\boldsymbol{\varepsilon}_{k+1}]|} \cdot \sum_{i=1}^{N'} w^i_{k+1|k} U_{[\mathbf{x}^i_{k+1|k}]}(\mathbf{x}) d\mathbf{x} =$$
$$\sum_{i=1}^{N'} \frac{w^i_{k+1|k}}{|[\mathbf{x}^i_{k+1|k}]| \cdot |[\boldsymbol{\varepsilon}_{k+1}]|} \int_{[\mathbf{x}^i_{k+1|k}]} |\,[\mathbf{z}] \cap (h_{k+1}(\mathbf{x}) + [\boldsymbol{\varepsilon}_{k+1}])\,|\, d\mathbf{x}$$
$$= \sum_{i=1}^{N'} \frac{w^i_{k+1|k}}{|[\boldsymbol{\varepsilon}_{k+1}]|} \frac{|[\tilde{\mathbf{x}}^i_{k+1}]|}{|[\mathbf{x}^i_{k+1|k}]|} \kappa^i_{k+1}. \tag{28}$$

The probability of existence is then updated as in (9). The $N' \times (m_k + 1)$ updated weights are then normalised to obtain $\tilde{w}^i_{k+1} = \tilde{w}^i_{k+1} / \sum_{j=1}^{N'} \tilde{w}^j_{k+1}$. Finally, we resample N times from $\{\tilde{w}^i_{k+1}, [\tilde{\mathbf{x}}^i_{k+1|k}]\}_{i=1}^{N' \times (m_k+1)}$ to obtain the new set of box particle $\{w^i_{k+1} = \frac{1}{N}, [\mathbf{x}^i_{k+1}]\}_{i=1}^{N}$. In addition here, as presented in [17], instead of duplicating box particles (sampled more than once in the resampling step), subdivision steps are used. Several strategies of subdivision can be used (e.g according the largest box face). In this paper we randomly pick a dimension for the selected box particle. The filter reports the posterior probability of existence $q_{k+1|k+1}$ and the box particle approximation of the posterior spatial PDF $s_{k+1|k+1}(\mathbf{x})$.

Remark 4: In [17], using the box particles at time $k+1$, an estimate can be obtained using the centre of the weighted box particles according to

$$\hat{\mathbf{x}}_{k+1} = \sum_{i=1}^{N} \omega^i_{k+1} \mathbf{c}^i_{k+1} \tag{29}$$

where $\mathbf{c}^i_{k+1}$ is the center of the i-th box particle.

VI. Numerical examples

A. Simulation setup

Consider the problem of tracking a target in a two-dimensional plane using range, range-rate and azimuth measurements. The target state vector is $\mathbf{x} = \begin{bmatrix} x & \dot{x} & y & \dot{y} \end{bmatrix}^\intercal$, where (x, y) and $(\dot{x}, \dot{y})$ are target position and velocity, respectively, in Cartesian coordinates. The target is moving according to the nearly constant velocity motion model with transitional density $\pi_{k+1|k}(\mathbf{x}|\mathbf{x}') = \mathcal{N}(\mathbf{x}; \mathbf{F}\mathbf{x}', \mathbf{Q})$. Here

$$\mathbf{F} = \mathbf{I}_2 \otimes \begin{bmatrix} 1 & T \\ 0 & 1 \end{bmatrix}, \quad \mathbf{Q} = \mathbf{I}_2 \otimes \begin{bmatrix} \frac{T^3}{3} & \frac{T^2}{2} \\ \frac{T^2}{2} & T \end{bmatrix} \cdot \varpi, \tag{30}$$

with $\otimes$ being the Kronecker product, $T = t_{k+1} - t_k$ the sampling interval and ϖ the intensity of process noise [16]. The target appears at scan $k = 3$ and disappears at scan $k = 54$. Initially (at $k = 0$) the target is located at $(550, 300)$m and is moving with velocity $(-5, -8.5)$m/s. The sensor is static, located at the origin of the $x - y$ plane. Other values are adopted as $\varpi = 0.05$, $T = 1$s, with the total observation interval of 60s.

The measurement function $h_k(\mathbf{x})$ is defined as:

$$h_k(\mathbf{x}) = \begin{bmatrix} \sqrt{x^2 + y^2} \\ \frac{x\dot{x} + \dot{y}y}{\sqrt{x^2+y^2}} \\ \arctan(y/x) \end{bmatrix}. \tag{31}$$

The measurement noise $\mathbf{v}$ is zero-mean white Gaussian with covariance $\boldsymbol{\Sigma} = \text{diag}[\sigma_r^2,\ \sigma_{\dot{r}}^2,\ \sigma_\theta^2]$, where $\sigma_r = 2.5$m, $\sigma_{\dot{r}} = 0.01$m/s and $\sigma_\theta = 0.25°$. The sensors provides interval measurements, with interval length $\boldsymbol{\Delta} = [\Delta r,\ \Delta \dot{r},\ \Delta\theta]^\intercal$, where $\Delta r = 50$m, $\Delta \dot{r} = 0.2$m/s and $\Delta\theta = 4°$ are the lengths of intervals in range, range-rate and azimuth, respectively.

The sensor has a bias (systematic error) in the sense that the vector $h_k(\mathbf{x})+\mathbf{v}_k$ is not in the middle of the measurement interval. A measurement at k is defined as:

$$[\mathbf{z}]_k = [h_k(\mathbf{x}) + \mathbf{v}_k - \frac{3}{4}\mathbf{\Delta},\ h_k(\mathbf{x}) + \mathbf{v}_k + \frac{1}{4}\mathbf{\Delta}]. \quad (32)$$

The filter is ignorant of the bias.

The probability of detection is $p_D = 0.95$, the mean number of clutter detections per scan is $\lambda = 5$. The clutter detection spatial distribution $c([\mathbf{z}])$ is uniformly across the range (mid intervals from 30m to 700m), range-rate (mid intervals from -15 to $+15$m/s) and azimuth (mid intervals from $-\pi/2$ to $\pi/2$rad).

The filtering algorithm knows a priori the following: p_D, clutter statistics λ and $c([\mathbf{z}])$, measurement function $h_k(\mathbf{x})$, covariance $\mathbf{\Sigma}$ and the transitional density $\pi_{k+1|k}(\mathbf{x}|\mathbf{x}')$. The filter is making inference at every k using measurements $\mathbf{\Upsilon}_{1:k}$, and the following parameters: $p_B = 0.01$, $p_S = 0.98$, $n_0 = 1$ and $N = 16$.

The experiment is implemented using MATLAB. Furthermore, the so called toolbox INTLAB [24] is used for the interval calculations.

Figure 1(a) shows a global view of the filter performance for one single run with measurements as described in (32). All the measurements for 60 scans are represented (rectangular regions around the sensor). In addition, the blue "plus" marks represent the true target trajectory, while the black cirles represent the estimated trajectory. The persistent box particles positions are also shown with rectangular regions. From this snapshot, we can see two interesting properties shown by the persistent box particles over the time: firstly, the update step is able to correctly weight the relevant box particles and secondly, the contraction steps combined with the resampling-subdivision steps helps reducing the size of the box particles over the time. From Figure 1(a), one can observe that this second property gives a visual convergence effect for the algorithm.

Figure 1(b) shows the estimate of the probability of target existence $q_{k|k}$ over time. Target presence is established at $k = 6$ with $q_{k|k}$ remaining close to 1.0 after that. Occasionally, when the target detection is missing in the measurement set $\mathbf{\Upsilon}_k$, $q_{k|k}$ drops below the value of 1.0.

B. Monte Carlo runs

The average performance of the proposed box particle Bernoulli filter has been validated via Monte Carlo simulations using the scenario and parameters described in Section VI-A (remark that the randomness comes essentially from both the resampling and the subdivision steps). Figure 2 shows: (a) the mean square error for the target position; (b) the mean square error for the target velocity. Averaging was carried out over $M = 100$ independent Monte Carlo runs with $N = 16$ box particles. From Figure 2 (a) and (b) one can observe the convergence and the very attractive potential of the Box particle to accurately estimate the target state with a very small cloud (in comparison to the thousands of particles usually necessary to correctly represents the posteriors).

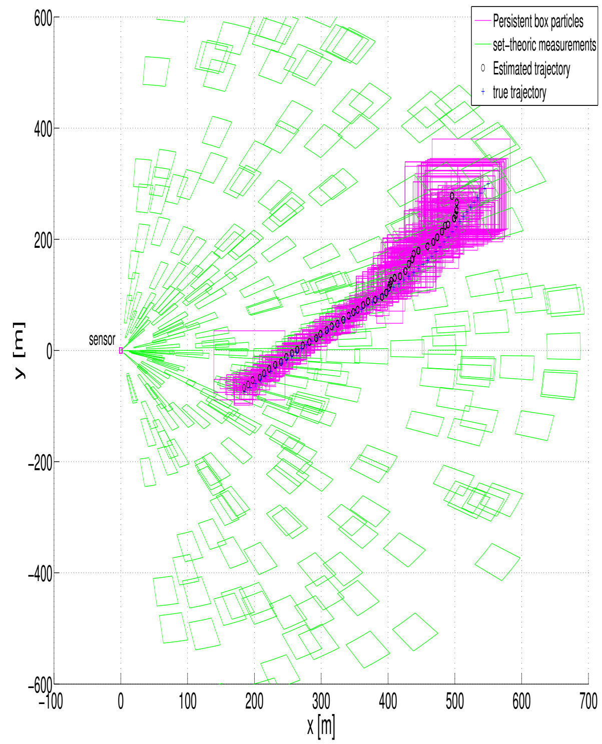

(a)

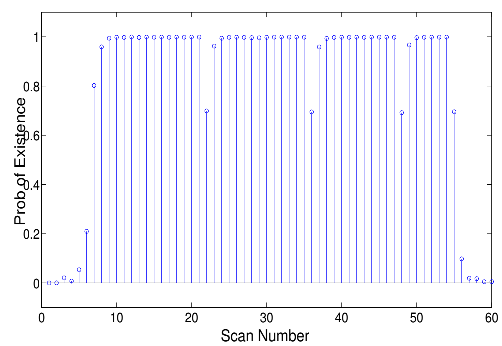

(b)

Figure 1. (a) Snapshot of one run (60 scans) of the box particles Bernouilli filter. The persistent box particles over the time are shown along with the estimated trajectory and the true one. (b) The estimate of the probability of target existence is also shown for one run.

VII. Summary and Future Work

The paper presented a box particle filter implementation of the Bernoulli filter for measurements affected by three sources of uncertainty: stochastic, set-theoretic and data association uncertainty. The filter efficiency is demonstrated using numerical simulations and it is shown to perform remarkably well: both the target existence and the target state are estimated reliably using a very small number of particles.

In the accompanying paper [23] an implementation of the

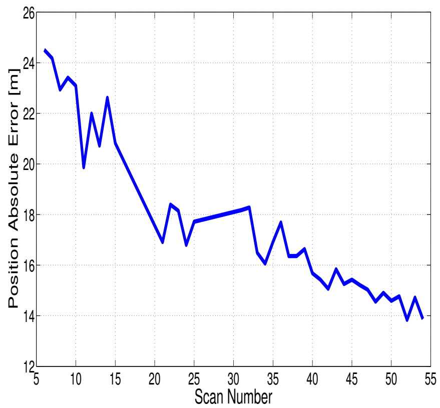

(a)

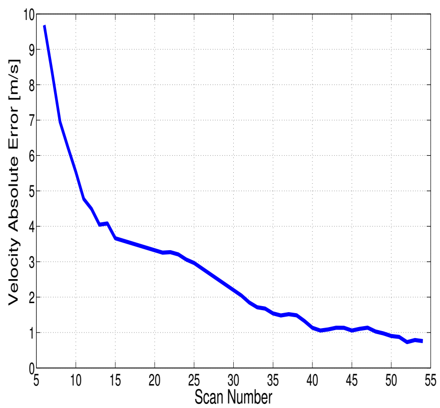

(b)

Figure 2. Error performance of the Bernoulli box particle filter (averaged over M = 100 independent Monte Carlo runs) using N = 16 box particles: (a) the mean square error for the target position; (b) the mean square error for the target velocity.

Bernoulli filter for measurements affected by three sources of uncertainty using particle filtering is investigated. A detailed comparison between the two filters would be useful to investigate in the future.

Acknowledgements. We acknowledge the support of the EPSRC project EP/E027253/1 and from the [European Community's] Seventh Framework Programme [FP7/2007-2013] under grant agreement No 238710 (Monte Carlo based Innovative Management and Processing for an Unrivalled Leap in Sensor Exploitation).

REFERENCES

[1] R. Mahler, *Statistical Multisource Multitarget Information Fusion*. Artech House, 2007.

[2] A. H. Jazwinski, *Stochastic Processes and Filtering Theory*. Academic Press, 1970.

[3] P. L. Combettes, "Foundations of set theoretic estimation," *Proc. IEEE*, vol. 81, no. 2, pp. 182–208, 1993.

[4] R. Kruse, E. Schwecke, and J. Heinsohn, *Uncertainty and vagueness in knowledge based systems*. Berlin: Springer-Verlag, 1991.

[5] P. Smets, "Imperfect information: Imprecision and uncertainty," in *Uncertainty Management in Information Systems*, 1996, pp. 225–254.

[6] G. J. Klir and M. J. Wierman, *Uncertainty-based information: Elements of generalized information theory*, 2nd ed. New York: Physica-Verlag, 1999.

[7] V. Klumpp, B. Noack, M. Baum, and U. D. Hanebeck, "Combined set-theoretic and stochastic estimation: A comparison of the SSI and CS filter," in *Proc. 13th Int. Conf. Information Fusion*, Edinburgh, UK, July 2010.

[8] A. Benavoli and A. Antonucci, "Aggregating imprecise probabilistic knowledge," in *Proc. 6th International Symposium on Imprecise Probability*, Durham, UK, 2009.

[9] S. M. Kay, *Fundamentals of Statistical Signal Processing: Detection theory*. Prentice Hall, 1998.

[10] B.-T. Vo, "Random finite sets in multi-object filtering," Ph.D. dissertation, School of EECE, The University of Western Australia, June 2008.

[11] R. Mahler, "The multisensor PHD filter II: Errorneous solution via "Poisson magic"," in *Proc. SPIE*, vol. 7336, 2009.

[12] A. Doucet, J. F. G. de Freitas, and N. J. Gordon, Eds., *Sequential Monte Carlo Methods in Practice*. New York: Springer, 2001.

[13] B. Ristic, S. Arulampalam, and N. Gordon, *Beyond the Kalman filter: Particle filters for tracking applications*. Artech House, 2004.

[14] D. Crisan and A. Doucet, "A survey of convergence results on particle filtering methods for practitioners," *IEEE Trans. Signal Processing*, vol. 50, no. 3, pp. 736–746, 2002.

[15] B. W. Silverman, *Density estimation for statistical and data analysis*. Chapman and Hall, 1986.

[16] Y. Bar-Shalom, X. R. Li, and T. Kirubarajan, *Estimation with Applications to Tracking and Navigation*. John Wiley & Sons, 2001.

[17] F. Abdallah, A. Gning, and P. Bonnifait, "Box particle filtering for nonlinear state estimation using interval analysis," *Automatica*, vol. 44, pp. 807–815, 2008.

[18] A. Gning, L. Mihaylova, and F. Abdallah, " Mixture of Uniform Probability Density Functions for non Linear State Estimation using Interval Analysis," *in Proc. 13th International Conference on Information Fusion*, Edinburgh, UK, 2010.

[19] L. Jaulin, M. Kieffer, O. Didrit and E. Walter, *Applied Interval Analysis*, Springer-Verlag, 2001.

[20] O. Cappé, A. Guillin, J. M. Marin, and C. P. Robert, "Population Monte Carlo," *Journal of Computational and Graphical Statistics*, vol. 13, no. 4, pp. 907–929, 2004.

[21] N. Oudjane and C. Musso, "Progressive correction for regularized particle filters," in *Proc. 3rd Int. Conf. Information Fusion*, Paris, France, 2000.

[22] R. E. Edwards. *What is the Riemann integral?* Dept. of Pure Mathematics, Dept. of Mathematics, Australian National University, Canberra, 1974.

[23] B. Ristic, A. Gning, and L. Mihaylova, "A Nonlinear filtering using measurements affected by stochastic, set-theoretic and association uncertainty," *in Proc. 14th International Conference on Information Fusion*, Chicago, US, 2011.

[24] S.M. Rump. "INTLAB - INTerval LABoratory", *in Tibor Csendes, editor, Developments in Reliable Computing*, pages 77-104. Kluwer Academic Publishers, Dordrecht, 1999.